



Research article

Barycentric rational interpolation method for solving KPP equation

Jin Li and Yongling Cheng*

School of Science, Shandong Jianzhu University, Jinan 250101, China

* **Correspondence:** Email: lijin@lsec.cc.ac.cn; Tel: +8618615186091.

Abstract: In this paper, we seek to solve the Kolmogorov-Petrovskii-Piskunov (KPP) equation by the linear barycentric rational interpolation method (LBRIM). As there are non-linear parts in the KPP equation, three kinds of linearization schemes, direct linearization, partial linearization, Newton linearization, are presented to change the KPP equation into linear equations. With the help of barycentric rational interpolation basis function, matrix equations of three kinds of linearization schemes are obtained from the discrete KPP equation. Convergence rate of LBRIM for solving the KPP equation is also proved. At last, two examples are given to prove the theoretical analysis.

Keywords: barycentric rational interpolation; collocation method; Kolmogorov-Petrovskii-Piskunov equation; non linear PDE

1. Introduction

Lots of physical phenomena can be expressed by non-linear partial differential equations (PDE) [1,2] and nonlinear Klein-Gordon equation [3], including inter alia, dissipative and dispersive PDE. In this paper, we consider the KPP equation

$$\frac{\partial \phi}{\partial t} - \frac{\partial^2 \phi}{\partial s^2} + \alpha \phi + \beta \phi^2 + \gamma \phi^3 = 0, 0 \leq s \leq 1, 0 \leq t \leq T, \gamma > 0 \quad (1.1)$$

$$\phi(0, t) = 0, \phi(1, t) = 0, 0 < t < T \quad (1.2)$$

where $\alpha, \beta, \gamma \in R$ are constant.

The KPP equation (1.1) was named after the Russian mathematicians Kolmogorov, Petrovsky, and Piskunov.

In the work of [4], modified extended tanh method was used to solve the KPP equation, and linear finite difference (FD) methods were presented to investigate numerical solution of the KPP equation. Furthermore, stability of the numerical scheme was proved. Explicit FD schemes [5] for the classical

Fisher KPP equation were explored, and stability analysis of the FD schemes was proved under choices of the model and numerical parameters. Generalized Fisher-KPP equation is solved by semi-explicit and implicit FD method [6], and stability and convergence of the proposed semi-explicit and implicit methods were also given, respectively. Based on the classical C-N scheme, classical Fisher-KPP equation [7] was studied, second-order accurate numerical estimates of time and space were obtained, and then stability, consistency, and (therefore) convergence of the proposed method were shown. Radially symmetric solutions of the generalized Fisher-KPP equation were presented in [8], analytical prediction was provided for the Heaviside equation. Multiple-term fractional KPP equation was investigated by Lie symmetry analysis method. Convergence analysis of exact power series solutions was also proposed in [9]. In [10], the fractional KPP equation was solved by q-homotopy analysis transform method (q-HATM), then uniqueness and convergence analysis of q-HATM the projected problem was also presented. In [11], numerical integration of the reproducing kernel gradient smoothing integration were constructed and the existence, uniqueness and error estimates of the solution of Galerkin meshless methods were established. In reference [12], recursive moving least squares (MLS) approximation was constructed in meshless methods. Properties and theoretical error of the recursive MLS approximation are analyzed.

In order to avoid the Runge phenomenon, lots of methods have been developed to overcome it. Among them, barycentric interpolation was developed in the 1960s. In recent years, linear rational interpolation (LRI) was proposed by Floater et al. [13–15], and error of linear rational interpolation [16–18] was also proved. The barycentric interpolation collocation method (BICM) has been developed by Wang et al. [19, 20], and the algorithm of BICM has been used for linear and non-linear problems [21, 22]. In recent research, the Volterra integro-differential equation (VIDE) [23], heat equation (HE) [24], biharmonic equation (BE) [25], telegraph equation (TE) [26], fractional differential equations [27], generalized Poisson equations [28] and fractional reaction-diffusion equation [29] have been studied by the linear barycentric rational interpolation collocation method (LBRIM), and their convergence rates were also proved.

In this paper, LBRIM has been used to solve the KPP equation with the matrix equation, which can be obtained easily. By three kinds of linearization, including direct linearization, partial linearization and Newton linearization, the nonlinear part of the KPP equation is translated into the linear part. A matrix equation of the linearization scheme is constructed from the linear KPP equation. Then, convergence rate of LBRIM of the discrete KPP equation is also given. At last, two numerical examples are presented to validate our theoretical analysis.

2. Linearization for KPP equation

In the following, the KPP equation is changed into the linear equation by linearization scheme, including direct linearization, partial linearization and Newton linearization.

2.1. Direct linearization

In the following KPP equation, the nonlinear term $\beta\phi^2 + \gamma\phi^3$ is changed to $\beta\phi_0^2 + \gamma\phi_0^3$:

$$\frac{\partial\phi}{\partial t} - \frac{\partial^2\phi}{\partial s^2} + \alpha\phi + \beta\phi_0^2 + \gamma\phi_0^3 = 0, \quad (2.1)$$

Then we get the linear scheme as

$$\frac{\partial \phi_k}{\partial t} - \frac{\partial^2 \phi_k}{\partial s^2} + \alpha \phi_k = -\beta \phi_{k-1}^2 - \gamma \phi_{k-1}^3, a \leq s \leq b, 0 \leq t \leq T. \quad (2.2)$$

2.2. Partial linearization

By the partial linearization, nonlinear term $\beta \phi^2 + \gamma \phi^3$ is changed to $\phi(\beta \phi_0 + \gamma \phi_0^2)$:

$$\frac{\partial \phi}{\partial t} - \frac{\partial^2 \phi}{\partial s^2} + \alpha \phi + \phi(\beta \phi_0 + \gamma \phi_0^2) = 0 \quad (2.3)$$

Then, we have

$$\frac{\partial \phi_k}{\partial t} - \frac{\partial^2 \phi_k}{\partial s^2} + \alpha \phi_k + (\beta \phi_{k-1} + \gamma \phi_{k-1}^2) \phi_k = 0, a \leq s \leq b, 0 \leq t \leq T. \quad (2.4)$$

2.3. Newton linearization

For the nonlinear term, by the Taylor expansion $\beta \phi^2 + \gamma \phi^3 = (\beta \phi_0^2 + \gamma \phi_0^3) + (2\beta \phi_0 + 3\gamma \phi_0^2)(\phi - \phi_0)$, we have

$$\frac{\partial \phi}{\partial t} - \frac{\partial^2 \phi}{\partial s^2} + \alpha \phi + \phi(2\beta \phi_0 + 3\gamma \phi_0^2) = \beta \phi_0^2 + 2\gamma \phi_0^3. \quad (2.5)$$

Then, we have

$$\frac{\partial \phi_k}{\partial t} - \frac{\partial^2 \phi_k}{\partial s^2} + \alpha \phi_k + (2\beta \phi_{k-1} + 3\gamma \phi_{k-1}^2) \phi_k = \beta \phi_{k-1}^2 + 2\gamma \phi_{k-1}^3, \quad (2.6)$$

where $k = 1, 2, \dots, .$

3. Differentiation matrices of KPP equation

Interval $[a, b]$ is divided into $a = s_0 < s_1 < s_2 < \dots < s_{m-1} < s_m = b$, for uniform partition with $h_s = \frac{b-a}{m}$ and nonuniform partition to be the second kind of Chebyshev point $x = \cos((0 : m)' \pi / m)$, $t = \cos((0 : n)' \pi / n)$. Time $[0, T]$ is divided into $0 = t_0 < t_1 < t_2 < \dots < t_{n-1} < t_n = T$ and $h_t = \frac{T}{n}$ to be a uniform partition. Then, we take $\phi_{nm}(s, t)$ to approximate $\phi(s, t)$ as

$$\phi_{nm}(s, t) = \sum_{i=0}^m \sum_{j=0}^n r_i(s) r_j(t) \phi_{ij} \quad (3.1)$$

where $\phi_{ij} = \phi(s_i, t_j)$.

$$r_i(s) = \frac{\frac{w_i}{s - s_i}}{\sum_{j=0}^m \frac{w_j}{s - s_j}}, \quad r_j(t) = \frac{\frac{w_j}{t - t_j}}{\sum_{i=0}^n \frac{w_i}{t - t_i}} \quad (3.2)$$

is the barycentric interpolation basis [26], and

$$w_i = \sum_{k \in J_i} (-1)^k \prod_{j=k, j \neq i}^{k+d_s} \frac{1}{s_i - s_j}, \quad w_j = \sum_{k \in J_j} (-1)^k \prod_{i=k, k \neq j}^{k+d_i} \frac{1}{t_j - t_i} \quad (3.3)$$

where $J_i = \{k \in I, i - d_s \leq k \leq i\}$, $I = \{0, 1, \dots, m - d_s\}$ (see [26]). We get the barycentric rational interpolation method (BRIM).

For the case

$$w_i = \frac{1}{\prod_{i \neq k} (s_i - s_k)}, \quad w_j = \frac{1}{\prod_{j \neq k} (t_j - t_k)}, \quad (3.4)$$

we get the barycentric Lagrange interpolation methods (BLIM).

So

$$r'_j(s_i) = \frac{w_j/w_i}{s_i - s_j}, \quad j \neq i, \quad r'_i(s_i) = - \sum_{j \neq i} r'_j(s_i), \quad (3.5)$$

$$r''_j(s_i) = k \left(r'_i(s_i) r'_i(s_j) - \frac{r'_i(s_j)}{s_i - s_j} \right), \quad j \neq i, \quad (3.6)$$

$$r''_i(s_i) = - \sum_{j \neq i} r''_j(s_i) \quad (3.7)$$

Then, we have

$$D_{ij}^{(0,1)} = r'_i(t_j), \quad (3.8)$$

$$D_{ij}^{(1,0)} = r'_i(s_j), \quad (3.9)$$

$$D_{ij}^{(2,0)} = r_i^{(2)}(s_j). \quad (3.10)$$

3.1. Matrix equation of direct linearization

Combining (3.1) and (2.2), we have

$$\left[\mathcal{I}_m \otimes \mathcal{D}^{(0,1)} + \mathcal{D}^{(2,0)} \otimes \mathcal{I}_n + \alpha \mathcal{I}_m \otimes \mathcal{I}_n \right] \phi_k = -\text{diag}(\beta \phi_{k-1}^2 + \gamma \phi_{k-1}^3), \quad (3.11)$$

and then we have

$$\mathcal{L} \phi_k = \Psi_{k-1} \quad (3.12)$$

where

$$\mathcal{L} = \mathcal{I}_m \otimes \mathcal{D}^{(0,1)} + \mathcal{D}^{(2,0)} \otimes \mathcal{I}_n + \alpha \mathcal{I}_m \otimes \mathcal{I}_n, \\ \Psi_{k-1} = -\text{diag}(\beta \phi_{k-1}^2 + \gamma \phi_{k-1}^3),$$

and \otimes is the Kronecher product [24].

3.2. Matrix equation of partial linearization

Combining (3.1) and (2.4), we have

$$\left[\mathcal{I}_m \otimes \mathcal{D}^{(0,1)} + \mathcal{D}^{(2,0)} \otimes \mathcal{I}_n + \alpha \mathcal{I}_m \otimes \mathcal{I}_n + \text{diag}(\beta \phi_{k-1}^2 + \gamma \phi_{k-1}^3) \right] \phi_k = 0, \quad (3.13)$$

$n = 1, 2, \dots$, and then we have

$$\mathcal{L} \phi_k = 0 \quad (3.14)$$

where $\mathcal{L} = \mathcal{I}_m \otimes \mathcal{D}^{(0,1)} + \mathcal{D}^{(2,0)} \otimes \mathcal{I}_n + \alpha \mathcal{I}_m \otimes \mathcal{I}_n + \text{diag}(\beta \phi_{k-1}^2 + \gamma \phi_{k-1}^3)$.

3.3. Matrix equation of Newton linearization

Combining (3.1) and (2.6), we have

$$\begin{aligned} & \left[\mathcal{I}_m \otimes \mathcal{D}^{(0,1)} + \mathcal{D}^{(2,0)} \otimes \mathcal{I}_n + \alpha \mathcal{I}_m \otimes \mathcal{I}_n + \text{diag}(2\beta \phi_{k-1}^2 + 3\gamma \phi_{k-1}^3) \right] \phi_k \\ & = \text{diag}(\beta \phi_{k-1}^2 + \gamma \phi_{k-1}^3), \end{aligned} \quad (3.15)$$

and then we get

$$\mathcal{L} \phi_k = \Psi_{k-1} \quad (3.16)$$

where

$$\mathcal{L} = \mathcal{I}_m \otimes \mathcal{D}^{(0,1)} + \mathcal{D}^{(2,0)} \otimes \mathcal{I}_n + \alpha \mathcal{I}_m \otimes \mathcal{I}_n + \text{diag}(2\beta \phi_{k-1}^2 + 3\gamma \phi_{k-1}^3),$$

and

$$\Psi_{n-1} = \text{diag}(\beta \phi_{k-1}^2 + \gamma \phi_{k-1}^3).$$

The boundary condition can be solved by substitution method, additional method or elimination method; see [20]. In the following, we adopt the substitution method and additional method.

4. Convergence rate of LBRIM for KPP equation

In this part, error estimate of KPP equation is given with $r_n(s) = \sum_{i=0}^n r_i(s) \phi_i$ to replace $\phi(s)$, where $r_i(s)$ is defined as in (3.2), and $\phi_i = \phi(s_i)$. We also define

$$e(s) := \phi(s) - r_n(s) = (s - s_i) \cdots (s - s_{i+d}) \phi [s_i, s_{i+1}, \dots, s_{i+d}, s]. \quad (4.1)$$

Then, we have the following.

Lemma 1. For $e(s)$ defined by (4.1) and $\phi(s) \in C^{d+2}[a, b]$,

$$|e^{(k)}(s)| \leq Ch^{d-k+1}, k = 0, 1, \dots. \quad (4.2)$$

For KPP equation, rational interpolation function of $\phi(s, t)$ is defined as $r_{mn}(s, t)$,

$$r_{mn}(s, t) = \frac{\sum_{i=0}^{m+d_s} \sum_{j=0}^{n+d_t} \frac{w_{i,j}}{(s-s_i)(t-t_j)} \phi_{i,j}}{\sum_{i=0}^{m+d_s} \sum_{j=0}^{n+d_t} \frac{w_{i,j}}{(s-s_i)(t-t_j)}} \quad (4.3)$$

where

$$w_{i,j} = (-1)^{i-d_s+j-d_t} \sum_{k_1 \in J_i} \prod_{h_1=k_1, h_1 \neq j}^{k_1+d_s} \frac{1}{|s_i - s_{h_1}|} \sum_{k_2 \in J_j} \prod_{h_2=k_2, h_2 \neq i}^{k_2+d_t} \frac{1}{|t_j - t_{h_2}|}. \quad (4.4)$$

We define $e(s, t)$ to be the error of $\phi(s, t)$ as

$$\begin{aligned} e(s, t) &:= \phi(s, t) - r_{mn}(s, t) \\ &= (s-s_i) \cdots (s-s_{i+d_s}) \phi[s_i, s_{i+1}, \dots, s_{i+d_s}, s, t] \\ &\quad + (t-t_j) \cdots (t-t_{j+d_t}) \phi[s, t_j, t_{j+1}, \dots, t_{j+d_t}, t]. \end{aligned} \quad (4.5)$$

With similar analysis to Lemma 1, we have the following.

Theorem 1. For $e(s, t)$ defined as (4.5) and $\phi(s, t) \in C^{d_s+2}[a, b] \times C^{d_t+2}[0, T]$, we have

$$|e^{(k_1, k_2)}(s, t)| \leq C(h_s^{d_s-k_1+1} + h_t^{d_t-k_2+1}), k_1, k_2 = 0, 1, \dots \quad (4.6)$$

We take the direct linearization of the KPP equation to prove the convergence rate. Let $\phi(s_m, t_n)$ be the approximate function of $\phi(s, t)$ and L be a bounded operator. Then,

$$L\phi(s_m, t_n) = 0, \quad (4.7)$$

and

$$\lim_{m, n \rightarrow \infty} L\phi(s_m, t_n) = 0. \quad (4.8)$$

Then, we get the following.

Theorem 2. For $\phi(s_m, t_n) : L\phi(s_m, t_n) = 0$ and L defined as (4.7),

$$|\phi(s, t) - \phi(s_m, t_n)| \leq C(h_s^{d_s-1} + \tau^{d_t}).$$

Proof. By (4.7), we have

$$\begin{aligned} &L\phi(s, t) - L\phi(s_m, t_n) \\ &= \frac{\partial \phi(s, t)}{\partial t} - \frac{\partial^2 \phi(s, t)}{\partial s^2} + \alpha \phi(s, t) + \beta \phi_0^2(s, t) + \gamma \phi_0^3(s, t) \\ &\quad - \left[\frac{\partial \phi(s_m, t_n)}{\partial t} - \frac{\partial^2 \phi(s_m, t_n)}{\partial s^2} + \alpha \phi(s_m, t_n) + \beta \phi_0^2(s_m, t_n) + \gamma \phi_0^3(s_m, t_n) \right] \\ &= \frac{\partial \phi}{\partial t} - \frac{\partial \phi}{\partial t}(s_m, t_n) + \frac{\partial^2 \phi}{\partial s^2} - \frac{\partial^2 \phi}{\partial s^2}(s_m, t_n) \\ &\quad + \left[\alpha \phi(s, t) + \beta \phi_0^2(s, t) + \gamma \phi_0^3(s, t) - (\alpha \phi(s_m, t_n) + \beta \phi_0^2(s_m, t_n) + \gamma \phi_0^3(s_m, t_n)) \right] \\ &:= E_1(s, t) + E_2(s, t) + E_3(s, t). \end{aligned} \quad (4.9)$$

Here

$$E_1(s, t) = \frac{\partial \phi}{\partial t} - \frac{\partial \phi}{\partial t}(s_m, t_n),$$

$$E_2(s, t) = \frac{\partial^2 \phi}{\partial s^2} - \frac{\partial^2 \phi}{\partial s^2}(s_m, t_n),$$

$$E_3(s, t) = \alpha \phi(s, t) + \beta \phi_0^2(s, t) + \gamma \phi_0^3(s, t) - (\alpha \phi(s_m, t_n) + \beta \phi_0^2(s_m, t_n) + \gamma \phi_0^3(s_m, t_n)).$$

For $E_2(s, t)$, we have

$$\begin{aligned} E_2(s, t) &= \frac{\partial^2 \phi}{\partial s^2} - \frac{\partial^2 \phi}{\partial s^2}(s_m, t_n) \\ &= \frac{\partial^2 \phi}{\partial s^2} - \frac{\partial^2 \phi}{\partial s^2}(s_m, t) + \frac{\partial^2 \phi}{\partial s^2}(s_m, t) - \frac{\partial^2 \phi}{\partial s^2}(s_m, t_n) \\ &= \frac{\sum_{i=0}^{m-d_s} (-1)^i \frac{\partial^2 \phi}{\partial s^2}[s_i, s_{i+1}, \dots, s_{i+d_1}, s_m, t]}{\sum_{i=0}^{m-d_s} \lambda_i(s)} \\ &\quad + \frac{\sum_{j=0}^{n-d_t} (-1)^j \frac{\partial^2 \phi}{\partial s^2}[t_j, t_{j+1}, \dots, t_{j+d_2}, s_m, t_n]}{\sum_{j=0}^{n-d_t} \lambda_j(t)} \\ &= \frac{\partial^2 e}{\partial s^2}(s_m, t) + \frac{\partial^2 e}{\partial s^2}(s_m, t_n). \end{aligned}$$

For $E_2(s, t)$, we get

$$|E_2(s, t)| \leq \left| \frac{\partial^2 e}{\partial s^2}(s_m, x) + \frac{\partial^2 e}{\partial s^2}(s_m, t_n) \right| \leq C(h^{d_s-1} + \tau^{d_t+1}). \quad (4.10)$$

Then, we have

$$|E_1(s, t)| \leq \left| \frac{\partial e}{\partial t}(s_m, t) + \frac{\partial e}{\partial t}(s_m, t_n) \right| \leq C(h^{d_s+1} + \tau^{d_t}). \quad (4.11)$$

Similarly, for $E_3(s, t)$ we have

$$|E_3(s, t)| \leq C(h^{d_s+1} + \tau^{d_t+1}). \quad (4.12)$$

Combining (4.9), (4.11), (4.12) together, the proof of Theorem 2 is completed.

5. Numerical examples

In this part, two examples are presented to test the theorem.

Example 1. Consider the KPP equation

$$\frac{\partial \phi}{\partial t} - \frac{\partial^2 \phi}{\partial s^2} + \alpha \phi + \beta \phi^2 + \gamma \phi^3 = 0$$

with the analysis solution

$$\phi(s, t) = -\frac{1}{3} - \frac{\sqrt{8+12b}}{3} + \sqrt{-2b} \tanh \left[\sqrt{-b} \left(s - \frac{\sqrt{8+12b}}{6} t \right) \right]$$

and under the condition $-8(1+6b)\sqrt{4+6b} - 11 = 0$, with the initial condition

$$\phi(s, 0) = -\frac{1}{3} - \frac{\sqrt{8+12b}}{3} + \sqrt{-2b} \tanh(\sqrt{-b}x)$$

and boundary condition

$$\phi(-40, t) = \phi_-, \phi(80, t) = \phi_+,$$

with $b = -\frac{3}{16} - \frac{\sqrt{5}}{16}$ and

$$\phi_- = \lim_{s \rightarrow -\infty} \left[-\frac{1}{3} - \frac{\sqrt{8+12b}}{3} + \sqrt{-2b} \tanh(\sqrt{-b}x) \right],$$

$$\phi_+ = \lim_{s \rightarrow \infty} \left[-\frac{1}{3} - \frac{\sqrt{8+12b}}{3} + \sqrt{-2b} \tanh(\sqrt{-b}x) \right].$$

In Figures 1–3, errors of direct linearization, partial linearization, Newton linearization with $m = n = 10$, $d_s = d_t = 7$ for the KPP equation by rational interpolation collocation methods are presented, respectively. From the figures, we know that the precision can reach to 10^{-10} for three kinds of linearization.

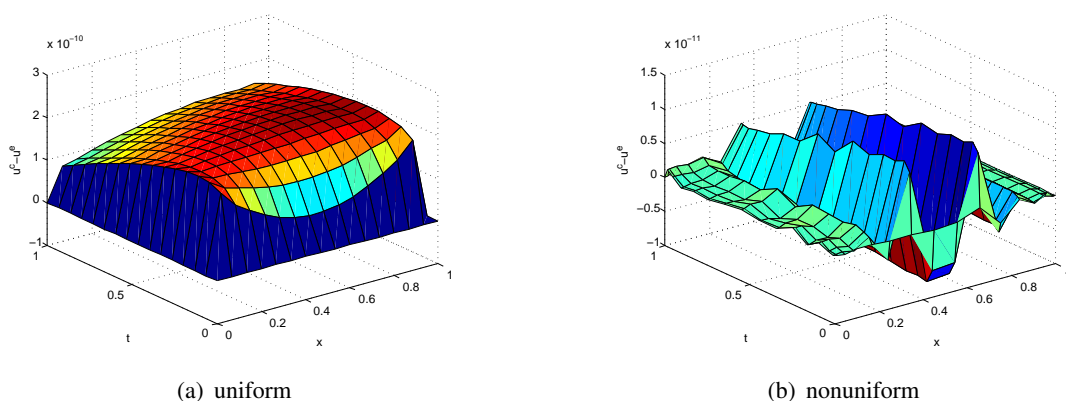


Figure 1. Errors of direct linearization with $m = n = 16$, $d_1 = d_2 = 7$, $[a, b] = [0, 1]$ in Example 4.1. (a) uniform, (b) nonuniform.

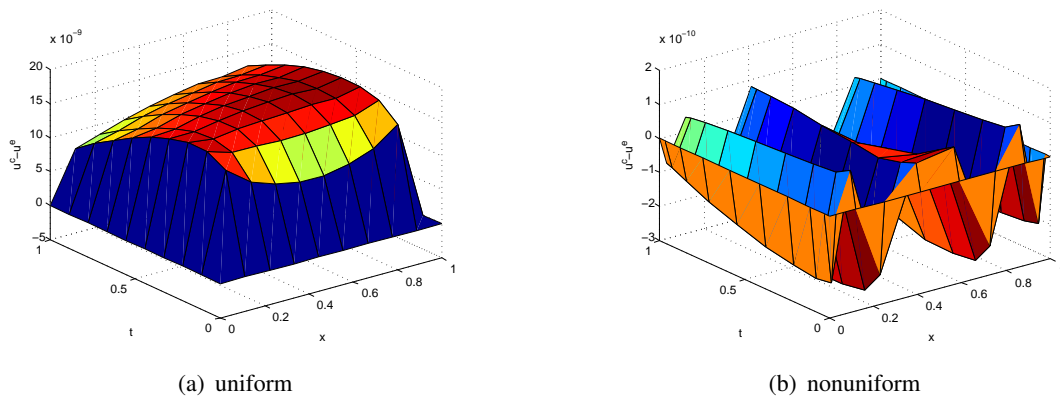


Figure 2. Errors of partial linearization with $m = n = 10$, $d_1 = d_2 = 7$, $[a, b] = [0, 1]$ in Example 4.1. (a) uniform, (b) nonuniform.

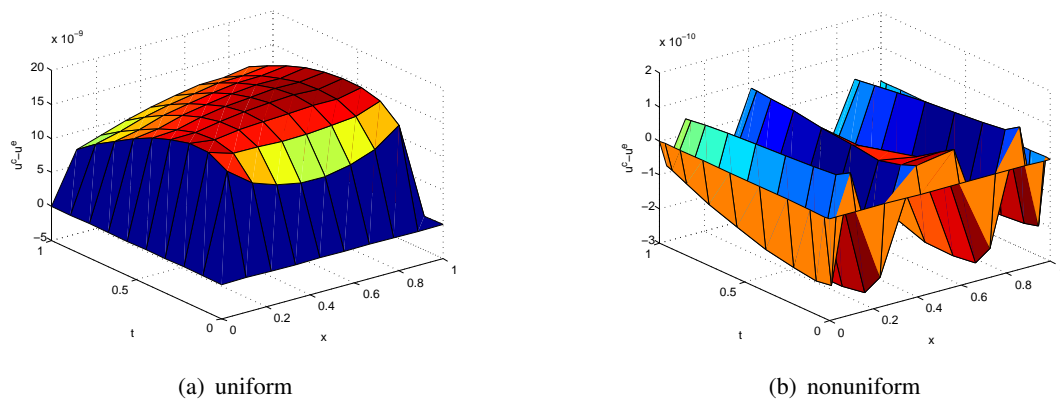


Figure 3. Errors of Newton linearization with rational $m = n = 10$, $d_1 = d_2 = 7$ in Example 4.1. (a) uniform, (b) nonuniform.

Table 1. Iteration ordinal number of BLIM and LBRIM for KPP equation with $m = n = 12$.

linearization	LBIM		LBRIM					
	uniform	nonuniform	uniform	nonuniform				
direct	4.3391e-11	9	1.6098e-11	9	3.1678e-09	9	1.5768e-10	9
partial	4.3557e-11	10	3.6622e-12	10	3.1678e-09	10	1.5770e-10	10
Newton	4.3636e-11	5	1.0834e-12	5	3.1678e-09	5	1.5772e-10	5

In Table 1, iteration ordinal numbers of BLIM and LBRIM for KPP equation with $m = n = 12$ are presented under $e = 10^{-10}$, while the boundary condition deals with the method of substitution. From Table 1, we know that iteration ordinal number of Newton linearization is less than other direct linearization methods and partial linearization.

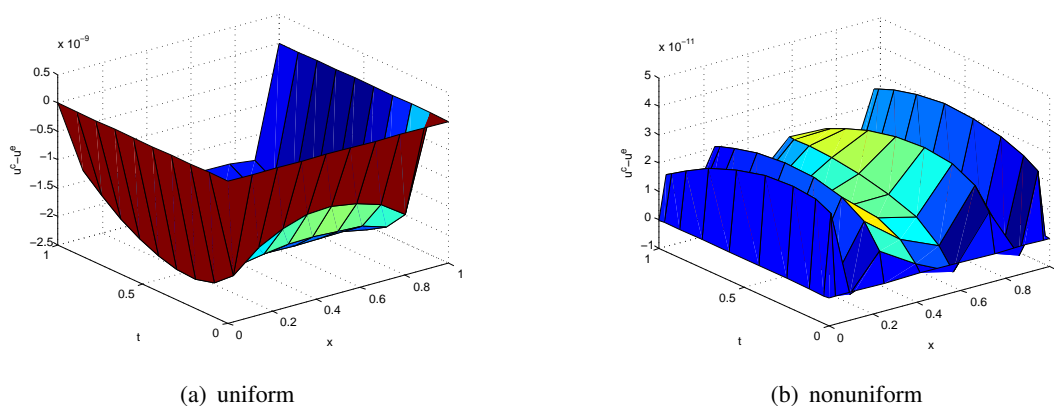


Figure 4. Errors of Newton linearization with LBCM $m = n = 10$, in Example 4.1. (a) uniform, (b) nonuniform.

In Figure 4, errors of Newton linearization with LBCM $m = n = 10$ for KPP equation by Lagrange interpolation collocation methods are presented. Compared with Newton linearization under rational interpolation collocation method, we can also get high accuracy. From Figure 4, we know that the precision can also reach 10^{-10} for uniform and nonuniform mesh.

Table 2. Errors of Newton linearization for α, β, γ under uniform with $m = n = 12$, $d_s = d_t = 9$.

	$\alpha = -\beta = -1$	$\beta = -\gamma = 1$	$\alpha = -\gamma = -1$
-5	2.4195e-08	2.7605e-10	2.9706e-10
-2	1.4645e-11	1.1929e-11	4.3791e-11
1	6.2681e-12	1.0389e-11	6.2681e-12
2	4.5979e-12	2.2771e-12	2.2429e-12
5	4.7751e-12	1.3827e-12	3.7885e-12

In Table 2, errors of Newton linearization for α, β, γ under uniform with $m = n = 12$, $d_s = d_t = 9$ are presented. In the first column, with $\alpha = -\beta = -1$, errors for $\gamma = -5, -2, 1, 2, 5$ are presented and can reach 10^{-12} . Meanwhile, for the second and third column, errors for $\alpha, \beta = -5, -2, 1, 2, 5$ are presented respectively, and the accuracy can also reach 10^{-12} .

In the following example, we take $\alpha = -1, \beta = 1, \gamma = 1$ to test our numerical algorithm.

Table 3. Errors of BLIM for KPP equation with $m = n = 16$.

	method of substitution		additional method	
	uniform	nonuniform	uniform	nonuniform
linearization				
direct	6.7391e-09	5.9533e-12	1.7651e-10	2.7792e-12
partial	4.0553e-09	1.3818e-11	3.1325e-10	1.3701e-11
Newton	5.2930e-09	3.6027e-12	3.5777e-11	8.2138e-14

In Tables 3 and 4, by BLIM and LBRIM, three kinds of linearization methods, direct, partial and

Newton linearization, are used to solve the KPP equation with boundary condition dealing with the method of substitution and the additional method, respectively. Errors show that the precisions under uniform and nonuniform are all the same with $m = n = 16$ in Table 3 and $m = n = 16, d_s = d_t = 7$ in Table 4.

Table 4. Errors of LBRIM for KPP equation with $m = n = 16, d_s = d_t = 7$.

	method of substitution		additional method	
	uniform	nonuniform	uniform	nonuniform
linearization				
direct	3.0396e-10	1.2940e-10	2.5244e-09	5.6023e-11
partial	3.1112e-10	1.3056e-10	2.5176e-09	5.7818e-11
Newton	3.7006e-10	1.3056e-10	2.5255e-09	5.5790e-11

Table 5. Errors of Newton linearization for t .

t	uniform		nonuniform	
	$(8, 8)d_s = d_t = 6$	$(16, 16)d_s = d_t = 12$	$(8, 8)d_s = d_t = 7$	$(16, 16)d_s = d_t = 15$
0.1	2.7194e-06	4.2786e-11	2.5418e-06	6.3038e-13
0.9	2.1531e-06	3.0908e-11	2.8847e-06	1.6875e-14
1	1.0817e-07	3.7229e-11	1.3454e-07	2.8311e-14
5	1.0162e-07	1.1727e-11	1.6906e-08	5.9952e-14
10	2.8122e-06	3.6257e-09	6.4357e-07	4.7354e-11
15	5.8758e-06	2.7142e-07	2.3034e-06	4.3082e-09

In Table 5, errors of Newton linearization for $t = 0.1, 0.9, 1, 5, 10, 15$ are presented under the uniform and nonuniform with $m = n = 8, 16$ and $d_s = d_t = 6, 12$, respectively. From Table 5, as the time variable becomes large, with proper choosing of m, n and d_s, d_t , the accuracy precision can reach 10^{-09} which means our method is still useful.

In the following table, direct linearization is chosen to present numerical results. From Tables 6 and 7, errors of direct linearization for uniform $d_t = 7$ with different d_s values are given, and the convergence rate is $O(h^{d_s} - 1)$. From Table 7, with space variable $s, d_s = 7$, the convergence rate is $O(h^{d_t})$, which agrees with our theorem.

Table 6. Errors of direct linearization for uniform for $d_t = 7$.

m, n	$d_s = 2$	h^α	$d_s = 3$	h^α	$d_s = 4$	h^α	$d_s = 5$	h^α
8	4.7077e-03		6.1377e-04		6.1907e-05		2.2449e-05	
12	2.4779e-03	1.5829	2.0398e-04	2.7168	1.4464e-05	3.5860	1.8462e-06	6.1612
16	1.8896e-03	0.9422	8.1190e-05	3.2023	6.9051e-06	2.5701	1.9952e-07	7.7340
20	1.5075e-03	1.0124	3.8071e-05	3.3939	3.0201e-06	3.7060	3.1135e-08	8.3246

Table 7. Errors of direct linearization for uniform for $d_s = 7$.

m, n	$d_t = 2$	τ^α	$d_t = 3$	τ^α	$d_t = 4$	τ^α	$d_t = 5$	τ^α
8	3.9953e-07		1.2610e-07		1.2893e-07		2.8790e-07	
12	1.6949e-07	2.1148	1.9734e-08	4.5744	8.3939e-10	12.416	8.8306e-10	14.272
16	8.9539e-08	2.2182	8.3374e-09	2.9950	1.0957e-10	7.0778	4.7227e-11	10.179
20	6.4086e-08	1.4988	5.1602e-09	2.1501	4.5771e-11	3.9117	8.6414e-12	7.6112

For Tables 8 and 9, the errors of Chebyshev partition for direct linearization with s and t are presented. For $d_t = 7$, the convergence rate is $O(h^{d_s})$ in Table 8, while in Table 9, the convergence rate is $O(h^{d_t})$, which agrees with our theorem.

Table 8. Errors of direct linearization for Chebyshev partition for $d_t = 7$.

m, n	$d_s = 2$	h^α	$d_s = 3$	h^α	$d_s = 4$	h^α	$d_s = 5$	h^α
8	1.9411e-03		3.2955e-04		5.7140e-05		2.0361e-05	
12	4.0048e-04	3.8927	4.5059e-05	4.9073	3.6799e-06	6.7641	1.1361e-07	12.797
16	2.2681e-04	1.9764	1.3156e-05	4.2793	2.6268e-07	9.1759	4.0012e-09	11.631
20	1.2927e-04	2.5195	8.7324e-06	1.8367	9.3088e-08	4.6489	7.9731e-10	7.2290

Table 9. Errors of direct linearization for Chebyshev partition for $d_s = 7$.

m, n	$d_t = 2$	τ^α	$d_t = 3$	τ^α	$d_t = 4$	τ^α	$d_t = 5$	τ^α
8	5.5468e-07		4.0183e-07		3.6812e-07		5.4111e-07	
12	8.3133e-08	4.6809	8.8031e-09	9.4236	7.5400e-10	15.268	4.1898e-10	17.668
16	4.5578e-08	2.0892	4.6599e-09	2.2111	3.3539e-11	10.820	2.6583e-11	9.5853
20	3.2921e-08	1.4578	2.5339e-09	2.7303	1.7307e-11	2.9649	1.6798e-12	12.376

In the following table, direct linearization is chosen to present numerical results. From Tables 10 and 11, errors of Newton linearization for uniform partition $d_t = 7$ with different d_s values are given, and the convergence rate is $O(h^{d_s} - 1)$. From Table 10, with space variable s , $d_s = 7$, the convergence rate is $O(h^{d_t})$, which agrees with our theorem.

Table 10. Errors of Newton linearization for uniform for $d_t = 7$.

m, n	$d_s = 2$	h^α	$d_s = 3$	h^α	$d_s = 4$	h^α	$d_s = 5$	h^α
8	4.3818e-03		6.1705e-04		6.2256e-05		2.2025e-05	
12	2.5447e-03	1.3402	2.0687e-04	2.6953	1.5769e-05	3.3868	1.8370e-06	6.1264
16	1.9287e-03	0.9635	8.1387e-05	3.2427	7.3540e-06	2.6515	1.8067e-07	8.0617
20	1.5338e-03	1.0268	3.8099e-05	3.4016	3.1384e-06	3.8160	2.6633e-08	8.5798

Table 11. Errors of Newton linearization for uniform for $d_s = 7$.

m, n	$d_t = 2$	τ^α	$d_t = 3$	τ^α	$d_t = 4$	τ^α	$d_t = 5$	τ^α
8	4.2023e-07		1.4489e-07		1.3869e-07		2.8207e-07	
12	1.7038e-07	2.2265	1.9678e-08	4.9238	8.4558e-10	12.578	9.3671e-10	14.077
16	8.9888e-08	2.2228	8.3237e-09	2.9908	1.1259e-10	7.0085	5.6174e-11	9.7813
20	6.3712e-08	1.5424	5.1515e-09	2.1503	4.6064e-11	4.0054	9.4698e-12	7.9785

For Tables 12 and 13, the errors of Chebyshev partition for Newton linearization with s and t are presented. For $d_t = 7$, the convergence rate is $O(h^{d_s})$ in Table 12, while in Table 13, the convergence rate is $O(h^{d_s})$, which agrees with our theorem.

Table 12. Errors of Newton linearization for Chebyshev partition for $d_t = 7$.

m, n	$d_s = 2$	h^α	$d_s = 3$	h^α	$d_s = 4$	h^α	$d_s = 5$	h^α
8	1.9012e-03		3.4523e-04		5.7649e-05		1.9973e-05	
12	4.0168e-04	3.8341	4.5180e-05	5.0154	3.6854e-06	6.7823	1.1597e-07	12.698
16	2.2820e-04	1.9655	1.3216e-05	4.2727	2.6512e-07	9.1488	3.1861e-09	12.495
20	1.2919e-04	2.5495	8.7313e-06	1.8577	8.1146e-08	5.3057	7.2055e-10	6.6618

Table 13. Errors of Newton linearization for Chebyshev partition for $d_s = 7$.

m, n	$d_t = 2$	τ^α	$d_t = 3$	τ^α	$d_t = 4$	τ^α	$d_t = 5$	τ^α
8	5.9248e-07		3.9805e-07		4.1713e-07		6.2982e-07	
12	8.4035e-08	4.8169	8.8160e-09	9.3966	4.0629e-10	17.102	4.4462e-10	17.895
16	4.4469e-08	2.2123	4.5532e-09	2.2968	3.0165e-11	9.0391	2.5477e-11	9.9396
20	3.2433e-08	1.4144	2.5000e-09	2.6867	1.6915e-11	2.5924	2.2268e-12	10.922

Example 2. Consider the KPP equation

$$\frac{\partial \phi}{\partial t} - \gamma \frac{\partial^2 \phi}{\partial s^2} - \phi + \phi^2 + \phi^3 = 0$$

with the initial condition

$$\phi(s, 0) = \sin(2\pi x), \quad x \in [0, 1],$$

and boundary condition

$$\phi(0, t) = \phi(1, t) = 0, \quad (0 \leq t \leq T).$$

In this example, there are no exact solutions under this initial condition and boundary condition. We take the error of iteration as $e = 10^{-10}$, and the numerical value of error of iteration is less than $e = 10^{-10}$, we get the numerical solution. Numerical solutions of direct linearization with $m = n = 19$, $d_1 = d_2 = 6$ under uniform and nonuniform partitions for $T = 0, T = 0.01, T = 0.02, T = 0.03, T = 0.04, T = 0.05$ are shown in Figure 5.

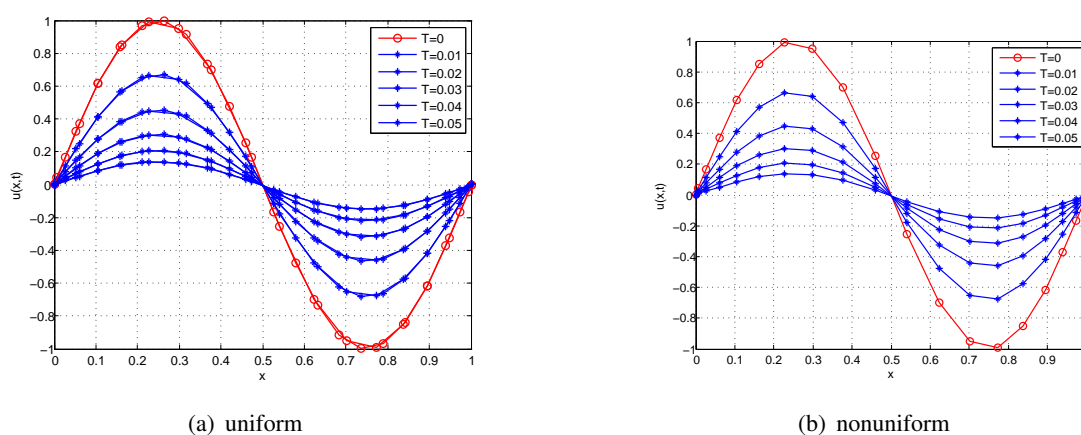


Figure 5. Numerical solutions of direct linearization with $m = n = 19$, $d_1 = d_2 = 6$, in Example 4.2. (a) uniform partition, (b) nonuniform partition.

6. Concluding remarks

In this paper, LBRIM is presented to solve (1+1) dimensional KPP equation. Three kinds of linearization methods are taken to translate the nonlinear part of the KPP equation into a linear part. A matrix equation of the discrete KPP equation is obtained from corresponding linearization schemes. Convergence rate of LBRIM is also presented. For the (2+1) or (3+1) dimensional KPP equation, the fractional time KPP equation can also be solved by LBRIM, we will investigate this case in the future paper.

Acknowledgments

The work of Jin Li was supported by the Natural Science Foundation of Shandong Province (Grant No. ZR2022MA003).

Conflicts of interest

The authors declare that they have no conflicts of interest.

References

1. Y. Liu, M. Song, H. Li, Y. Li, W. Hou, Containment problem of finite-field networks with fixed and switching topology, *Appl. Math. Comput.*, **411** (2021), 126519. <https://doi.org/10.1016/j.amc.2021.126519>
2. Y. Liu, Bifurcation techniques for a class of boundary value problems of fractional impulsive differential equations, *J. Nonlin. Sci. Appl.*, **8** (2015), 340–353. <https://doi.org/10.22436/JNSA.008.04.07>

3. D. Mehdi, S. Ali, Numerical solution of the nonlinear Klein-Gordon equation using radial basis functions, *J. Comput. Appl. Math.*, **230** (2009), 400–410. <https://doi.org/10.1016/j.cam.2008.12.011>
4. B. Wongsajjai, T. Aydemir, T. Ak, S. Dhawan, Analytical and numerical techniques for initial-boundary value problems of kolmogorov-petrovsky-piskunov equation, *Numer. Methods Partial Differ. Equations*, **2020** (2020), 1–18. <https://doi.org/10.1002/num.22693>
5. J. E. Macías-Díaz, A. Puri, An explicit positivity-preserving finite-difference scheme for the classical Fisher-Kolmogorov-Petrovsky-Piscounov equation, *Appl. Math. Comput.*, **218** (2012), 5829–5837. <https://doi.org/10.1016/j.amc.2011.11.064>
6. W. Qin, D. Ding, X. Ding, Two boundedness and monotonicity preserving methods for a generalized Fisher-KPP equation, *Appl. Math. Comput.*, **252** (2015), 552–567. <https://doi.org/10.1016/j.amc.2014.12.043>
7. M. Izadi, A second-order accurate finite-difference scheme for the classical Fisher-Kolmogorov-Petrovsky-Piscounov equation, *J. Inf. Optim. Sci.*, **42** (2021), 431–448. <https://doi.org/10.1080/02522667.2019.1696919>
8. J. E. Macías-Díaz, I. E. Medina-Ramírez, A. Puri, Numerical treatment of the spherically symmetric solutions of a generalized Fisher-Kolmogorov-Petrovsky-Piscounov equation, *J. Comput. Appl. Math.*, **231** (2009), 851–868. <https://doi.org/10.1016/j.cam.2009.05.008>
9. C. Y. Qin, S. F. Tian, X. B. Wang, L. Zou, T. T. Zhang, Lie symmetry analysis, conservation laws and analytic solutions of the time fractional Kolmogorov-Petrovskii-Piskunov equation, *Chin. J. Phys.*, **56** (2018), 1734–1742. <https://doi.org/10.1016/j.cjph.2018.05.002>
10. P. Veerasha, D. G. Prakasha, D. Baleanu, An efficient numerical technique for the nonlinear fractional Kolmogorov-Petrovskii-Piskunov equation, *Mathematics*, **7** (2019), 1–18. <https://doi.org/10.3390/math7030265>
11. X. L. Li, Theoretical analysis of the reproducing kernel gradient smoothing integration technique in galerkin meshless methods, *J. Comp. Math.*, **41** (2023), 503–526. <https://doi.org/10.4208/jcm.2201-m2021-0361>
12. J. Wan, X. L. Li, Analysis of a superconvergent recursive moving least squares approximation, *Appl. Math. Lett.*, **133**, (2022), 108223 <https://doi.org/10.1016/j.aml.2022.108223>
13. M. Floater, H. Kai, Barycentric rational interpolation with no poles and high rates of approximation, *Numer. Math.*, **107** (2007), 315–331. <https://doi.org/10.1007/s00211-007-0093-y>
14. G. Klein, J. Berrut, Linear rational finite differences from derivatives of barycentric rational interpolants, *SIAM J. Numer. Anal.*, **50** (2012), 643–656. <https://doi.org/10.1137/110827156>
15. G. Klein, J. Berrut, Linear barycentric rational quadrature, *BIT Numer. Math.*, **52** (2012), 407–424. <https://doi.org/10.1007/s10543-011-0357-x>
16. J. Berrut, S. Hosseini, G. Klein, The linear barycentric rational quadrature method for Volterra integral equations, *SIAM J. Sci. Comput.*, **36**, (2014), 105–123. <https://doi.org/10.1137/120904020>
17. P. Berrut, G. Klein. Recent advances in linear barycentric rational interpolation, *J. Comput. Appl. Math.*, **259** (2014), 95–107. <https://doi.org/10.1016/j.cam.2013.03.044>

18. E. Cirillo, K. Hormann, On the Lebesgue constant of barycentric rational Hermite interpolants at uniform partition, *J. Comput. Appl. Math.*, **349** (2019), 292–301. <https://doi.org/10.13140/RG.2.2.34932.65923>
19. S. Li, Z. Q. Wang, *High Precision Meshless barycentric Interpolation Collocation Method—Algorithmic Program and Engineering Application*, Science Publishing, 2012.
20. Z. Q. Wang, S. Li, *Barycentric Interpolation Collocation Method for Nonlinear Problems*, National Defense Industry Press, Beijing, 2015.
21. Z. Q. Wang, Z. K. Xu, J. Li, Mixed barycentric interpolation collocation method of displacement-pressure for incompressible plane elastic problems, *Chin. J. Appl. Mech.*, **35** (2018), 195–201. <https://doi.org/10.11776/cjam.35.03.D011>
22. Z. Q. Wang, L. Zhang, Z. K. Xu, J. Li, Barycentric interpolation collocation method based on mixed displacement-stress formulation for solving plane elastic problems, *Chin. J. Appl. Mech.*, **35** (2018), 304–309. <https://doi.org/10.11776/cjam.35.02.D002>
23. J. Li, Y. Cheng, Linear barycentric rational collocation method for solving second-order Volterra integro-differential equation, *Comput. Appl. Math.*, **39** (2020). <https://doi.org/10.1007/s40314-020-1114-z>
24. J. Li, Y. Cheng, Linear barycentric rational collocation method for solving heat conduction equation, *Numer. Methods Partial Differ. Equations*, **37** (2021), 533–545. <https://doi.org/10.1002/num.22539>
25. J. Li, Y. Cheng, Barycentric rational method for solving biharmonic equation by depression of order, *Numer. Methods Partial Differ. Equations*, **37** (2021), 1993–2007. <https://doi.org/10.1002/num.22638>
26. J. Li, Linear barycentric rational collocation method for solving biharmonic equation, *Demonstr. Math.*, **55** (2022), 587–603. <https://doi.org/10.1515/dema-2022-0151>
27. J. Li, X. N. Su, K. Y. Zhao, Barycentric interpolation collocation algorithm to solve fractional differential equations, *Math. Comput. Simul.*, **205** (2023), 340–367. <https://doi.org/10.1016/j.matcom.2022.10.005>
28. J. Li, Y. L. Cheng, Z. C. Li, Z. K. Tian, Linear barycentric rational collocation method for solving generalized Poisson equations, *Math. Biosci. Eng.*, **20** (2023), 4782–4797. <https://doi.org/10.3934/mbe.2023221>
29. J. Li, Barycentric rational collocation method for fractional reaction-diffusion equation, *AIMS Math.*, **8** (2023), 9009–9026. <https://doi.org/10.3934/math.2023451>



AIMS Press

©2023 the Author(s), licensee AIMS Press. This is an open access article distributed under the terms of the Creative Commons Attribution License (<http://creativecommons.org/licenses/by/4.0>)